MDPI

Communication

Effect of Batch-Annealing Temperature on Oxidation of 22MnB5 Steel during Austenitizing

Bibo Li [1,*], Yanning Liu [1], Ying Chen [1], Nan Li [1], Xiaolong Zhao [2], Jikang Li [1] and Maoqiu Wang [1]

1   Central Iron and Steel Research Institute Group, Beijing 100081, China
2   Jiuquan Iron and Steel Group Co., Ltd., Jiayuguan 735100, China
*   Correspondence: 15910936876@163.com; Tel.: +86-010-6218-1270

Abstract: In this paper, the effect of batch-annealing temperature on the oxidation of 22MnB5 steel during austenitizing was studied. When the batch-annealing temperature was decreased from 690 to 680 °C, the surface roughness of cold-rolled 22MnB5 steel decreased, which reduced the oxide layer thickness during the subsequent austenitizing process and had little effect on the mechanical properties in the cold-rolled and quenched state. This indicated that oxidation during austenitizing could be reduced by properly reducing the batch-annealing temperature without affecting the mechanical properties.

Keywords: hot stamping steel; batch-annealing temperature; oxidation; austenitizing; surface roughness

1. Introduction

Hot stamping is ideal for processing high-strength steel used in automotive structural parts [1–3]. During hot stamping, steel is subjected to high-temperature processes such as austenitizing, which make it prone to oxidation [4]. Oxide scales will increase the loss of steel, cause iron oxide to press into the steel surface, cause wear and tear on the die, and reduce the service life of hot stamping equipment [5]. Oxidation can often be decreased by adjusting the hot-stamping process [6,7], by alloying [8,9], or by using protective measures [10–12]. Zhao et al. [13] designed a new hot-stamping steel with a high Cr: Si ratio. A dense Cr/Si oxide layer was formed, which prevented oxygen ions from entering the steel surface for further oxidation. Mori et al. [14] observed that oxidation during hot stamping was prevented by coating sheets with oxidation-preventative oil. However, the influence of the original material (cold-rolled sheet) on oxidation during hot stamping was ignored. The production process of cold-rolled coils is hot rolling → pickling → cold rolling → batch annealing → leveling [15,16]. All-hydrogen batch annealing of cold rolling can eliminate the residual stress, obtain recrystallized grains, and obtain a bright and smooth surface [17,18]. Thus, changing the batch-annealing process will change the microstructure [19,20], mechanical properties [21,22], and surface roughness [23,24] after batch annealing; these, in turn, may affect the microstructure, mechanical properties, and the oxide decarburized layer after austenitizing. A hot-stamping parts production company found that the oxide scale in the hot-stamping process decreased when the initial cold-rolled sheet's batch-annealing temperature decreased. Therefore, the influence of batch annealing on oxidation and decarburization in the austenitizing process or hot stamping is worthy of attention. In this paper, the effect of the batch-annealing temperature during cold rolling on the microstructure, mechanical properties, and especially oxidation of 22MnB5 steel during subsequent austenitizing was studied, and its reasons for the difference in oxidation were also discussed.

2. Materials and Methods

The material used in this experiment was a 22MnB5 (C~0.24%, Mn~1.17%, Si~0.24%, Cr~0.25%, B~0.001%, wt.%) cold-rolled coil produced by a steel company. The cold-rolled sample #1 (batch-annealing temperature: 690 °C) and sample #2 (batch-annealing temperature: 680 °C) were obtained by adjusting the all-hydrogen batch-annealing temperature of the hard-rolled coil. The cold-spot temperatures of hard-rolled coils in batch annealing were set separately at 650 °C and 660 °C. The hot-spot temperatures were set at 680 °C and 690 °C, with a longer holding time (12 h). The hydrogen flow rate in the furnace was varied according to the needs, about 20–30 m^3/h. After the insulation was finished, the inner cover was cooled by an air blower to 380 °C and then the inner cover was cooled by water spraying. The annealing process was finished when the temperature was 50 °C. A schematic diagram of a batch-annealing furnace (EBNER, Linz, Austria) and cold and hot temperature curves are shown in Figure 1. Then, the cold-rolled samples were austenitized by holding at 920 °C for 5 min and then quenched in oil to obtain quenched samples #1 and #2.
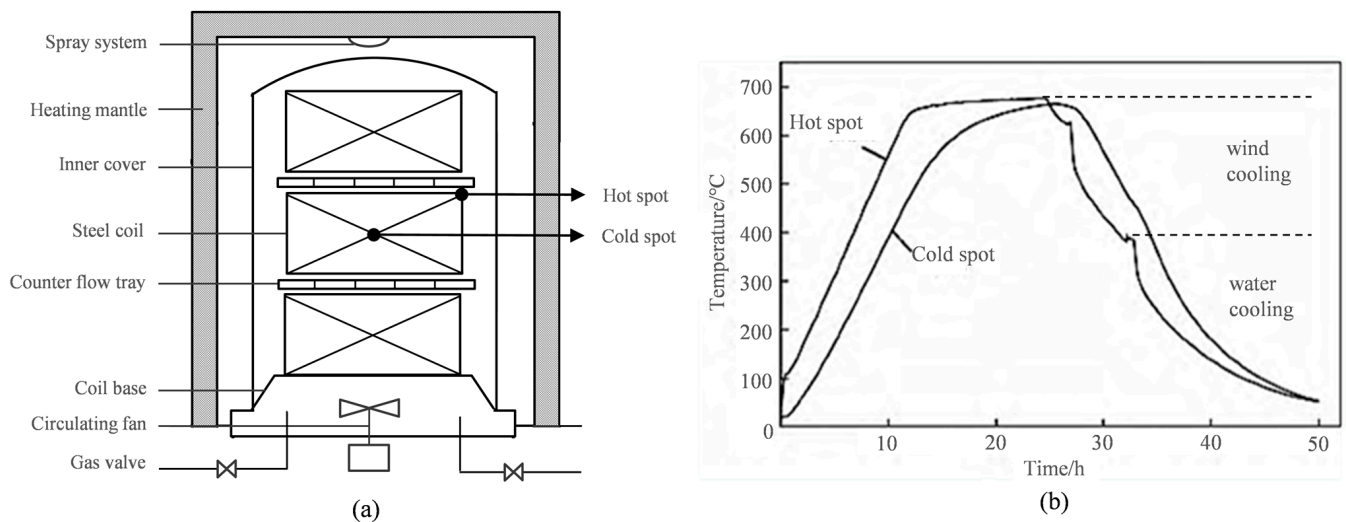

Figure 1. Schematic diagram of batch-annealing furnace (**a**) and cold and hot temperature curves (**b**).

The mechanical properties of cold-rolled and quenched samples were tested by an MTS universal testing machine (MTS Systems Inc., Eden Prairie, MN, USA), and the parallel section was 30 mm × 5 mm × 2 mm. The microstructures of cold-rolled and quenched samples were observed by optical microscopy (OM) (Leica, Vizsla, Germany). The surface morphology and roughness of the samples were observed by laser confocal microscopy (Lasertec, Yokohama, Japan). The oxidation weight gain curves of the samples were obtained by a thermos gravimetric analyzer (NETZSCH, Bavaria, Germany) in an alumina crucible. To reduce the errors, the balance was calibrated before the test, and blank curves were obtained according to the experimental conditions. All samples were tested in the same period, and each group of samples had three parallel samples. The samples were heated from room temperature to 920 °C at a rate of 20 °C/min and held at that temperature for 30 min. Samples were protected during heating by nitrogen gas with a flow rate of 100 mL/min, and the samples were oxidized by mixed air (N_2:O_2 = 4:1) during the heat-preservation process.

3. Results and Discussion

Figure 2 shows the morphology of the decarburized layer (Figure 2a,c) and oxide layer (Figure 2b,d) after holding at 920 °C for 5 min. The sample sections after heat treatment were inlaid by cold mounting. The oxide skin and the matrix are not tightly bound and easy to separate, so the resin enters the interface between the oxide skin and the matrix during cold mounting. The average thicknesses of the decarburized layers of quenched samples #1

and #2 were 21.9 µm and 20.1 µm, and the average thicknesses of the oxidized layers were 58.5 µm and 41.4 µm, respectively. When the batch-annealing temperature decreases from 690 to 680 °C, the average thicknesses of the decarburized layers of quenched #1 and #2 samples were not significantly different, while the average thickness of the oxide layer of quenched sample #1 was larger than that of sample #2. Thus, reducing the batch-annealing temperature had little effect on the decarburized layer of 22MnB5 steel, but it did reduce the thickness of the oxide layer, which is favorable for the hot stamping of bare sheets. In the next part of the study, we investigated the factors responsible for the different oxide-layer thicknesses of quenched samples #1 and #2.
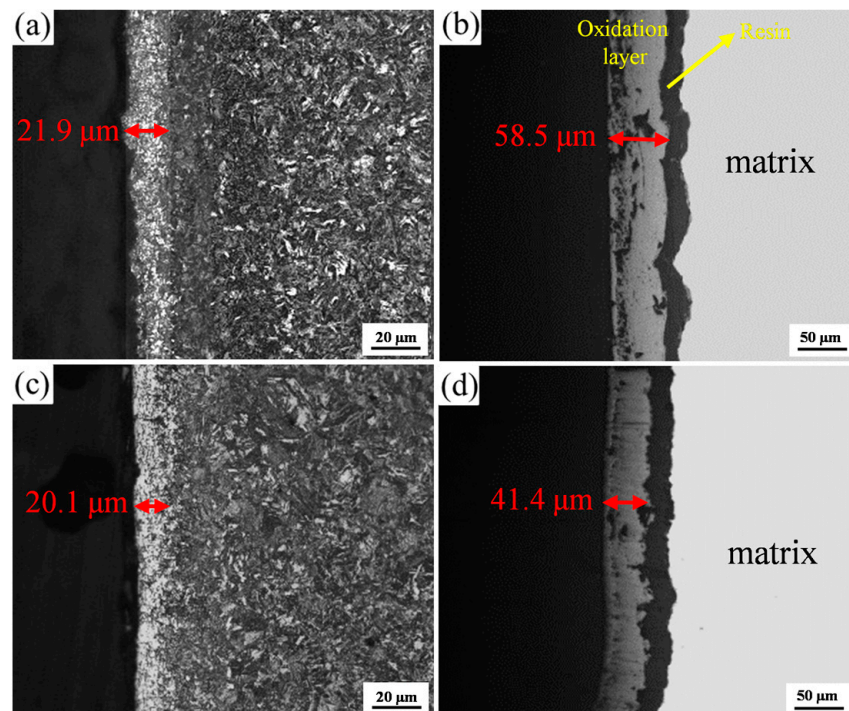

Figure 2. The morphology of the decarburized layer and oxide layer after holding at 920 °C for 5 min: (**a**,**b**) quenched sample #1; (**c**,**d**) as-quenched sample #2.

First, the effect of the batch-annealing temperature on the microstructure and mechanical properties of cold-rolled and quenched 22MnB5 steel was analyzed. Figure 3a,c show the cold-rolled microstructure of samples #1 and #2, which are composed of spherical pearlite and ferrite. Compared with sample #1, the spherical cementite in sample #2 occurred during segregation, which decreased the microstructure uniformity after cold rolling. This is because, after reducing the annealing temperature from 690 to 680 °C, the diffusion speed of the carbon in the cold-rolled #2 sample slowed down, and segregation of the cementite occurred during its formation due to slow diffusion. Figure 3b,d show the quenched structures of samples #1 and #2 after austenitizing. After quenching, there was little difference between the structure of samples #1 and #2, which were composed of fine lath martensite. This indicates that reducing the batch-annealing temperature from 690 to 680 °C has less effect on the microstructure of 22MnB5 steel after austenitizing.

The mechanical properties of cold-rolled and quenched samples #1 and #2 are shown in Figure 4. The ultimate tensile strength (UTS), yield strength (YS), and elongation of cold-rolled in sample #1 were 513 MPa, 331 MPa, and 33%, while for cold-rolled sample #2, the measurements were 512 MPa, 333 MPa, and 33%, respectively. It can be seen that although the microstructure uniformity of cold-rolled sample #2 decreased compared with that of sample #1, its mechanical properties were not decreased. The tensile strength and yield strength of quenched sample #2 were slightly increased to 1482 MPa and 1092 MPa, respectively, compared with that of quenched sample #1, which were 1467 MPa and

1092 MPa, while the elongations of both were 10%. Thus, when the batch-annealing temperature decreased from 690 to 680 °C, the mechanical properties of the cold-rolled and quenched samples changed only slightly, indicating that the mechanical properties are not affected by reducing the annealing temperature properly. To sum up, after reducing the batch-annealing temperature from 690 to 680 °C, the uniformity of the cold-rolled structure was reduced but had little effect on the cold-rolled and quenched mechanical properties of 22MnB5 steel.
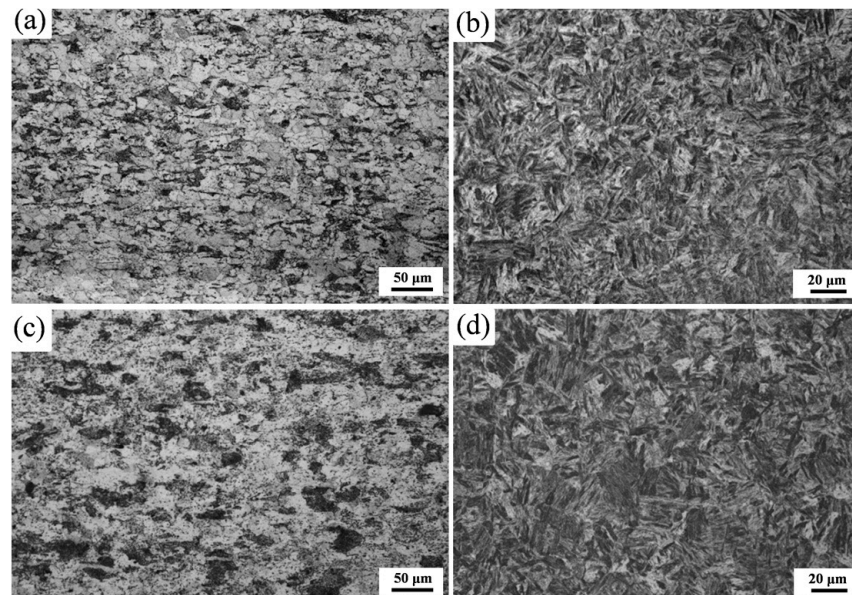

Figure 3. The cold-rolled (**a,c**) and quenched (**b,d**). Microstructure of samples #1 (**a,b**) and #2 (**c,d**).
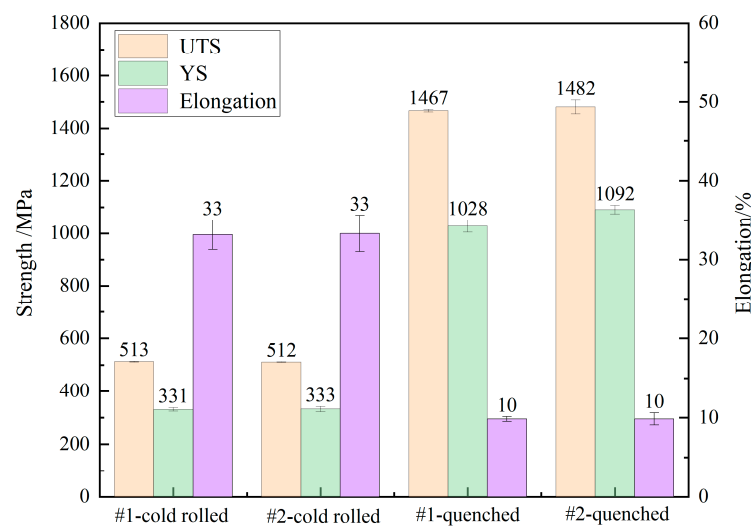

Figure 4. The mechanical properties of cold-rolled and quenched #1 and #2 samples.

The batch-annealing temperature may also affect the surface roughness of cold-rolled sheets. Next, the surface roughness and three-dimensional surface morphology of cold-rolled samples were analyzed, and the results are shown in Figure 5. Figure 5 shows that the linear roughness of cold-rolled samples #1 and #2 was 1.975 µm and 1.496 µm, respectively, and the fluctuation of the three-dimensional surface topography of sample #1 was greater than that of sample #2. Moreover, the surface roughness of cold-rolled samples #1 and #2 was 1.601 µm and 1.252 µm. Those results showed that properly reducing the batch-annealing temperature improved the surface quality of the cold-rolled coil and obtained a lower surface roughness. There are three main reasons for the influence of full

hydrogen batch-annealing temperature on the surface roughness of cold-rolled sheets. First, it will affect the oxidation-reduction effect of hydrogen on the surface metal of a hard-rolled coil [25]. Second, it will affect the release of internal stress and static recrystallization during batch annealing, which will cause grain rotation and local plastic deformation [26,27]. Third, the higher the annealing temperature, the greater the temperature difference and thermal stress, and the reduced iron powder is easier to bond on the surface of the steel plate, thus affecting surface roughness.
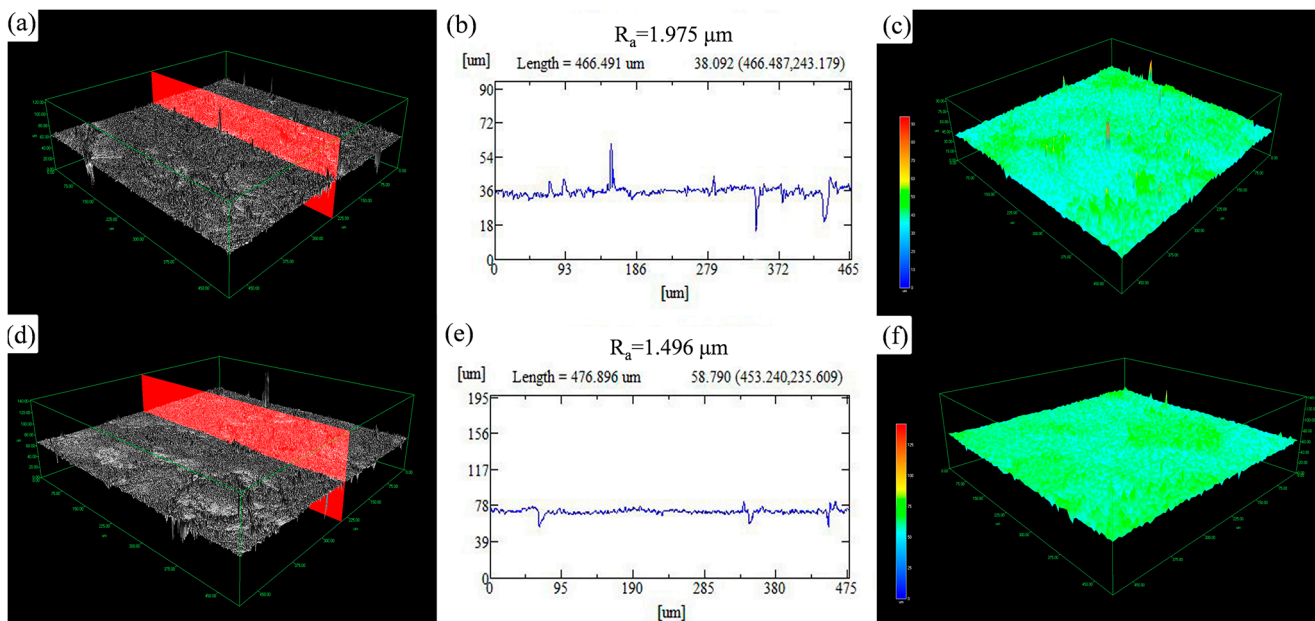

Figure 5. The linear roughness and three-dimensional surface morphology of 22MnB5 steel: (**a**–**c**) cold-rolled sample #1; (**d**–**f**) cold-rolled sample #2.

To further confirm the effect of surface roughness on oxidation during austenitizing, the oxidation weight gain curves of cold-rolled samples #1 and #2 and cold-rolled samples #1 and #2 polished with 600 mesh sandpaper were obtained by thermogravimetric analysis. The results are shown in Figure 6. After being polished with 600 mesh sandpaper, the surface roughness of the cold-rolled #1 and #2 samples was similar (2.215 μm and 2.289 μm, respectively), and the oxidation weight gain curves of the two samples almost coincided. The #1 and #2 cold-rolled samples polished with 600-mesh sandpaper have different microstructures but the same surface quality, while their oxidation weight gain curves almost coincide, indicating that slight microstructure difference caused by the reduction of the batch-annealing temperature will not cause oxidation differences when there is little difference in surface roughness. The oxidation weight gain of the unpolished cold-rolled #1 sample was greater than that of the #2 sample, showing that a higher surface roughness rather than microstructure differences increased the oxidation rate and oxidation weight gain, which is consistent with the experimental results in Figure 2. Therefore, these can prove that the difference in oxidation during austenitizing is caused by the difference in surface quality rather than the slight microstructure difference caused by an increase in batch-annealing temperature. The greater the surface roughness of the sample, the greater the surface fluctuations, the larger the actual surface area in contact with the air, and the more oxygen ions that can diffuse into the matrix. These will increase the oxidation intensity and result in a greater weight gain during oxidation [28]. As can be seen from the cross-section diagram of the oxide layer in Figure 1, the outer surfaces of the oxide layers of samples #1 and #2 were relatively smooth due to their relationship with interfacial energy. The oxide layer at the concave valley on the sample surface was thicker than that at the convex peak because the concave valley could absorb more oxygen ions and provide more diffusion channels [29]. The wavy morphology of the oxide layer increased the internal

stress of the oxide film, making it easier for cracks at the interface between the oxide film and matrix to expand [30,31]. Therefore, during oxidation, the oxide film on a rough surface was more likely to peel off than the oxide film on a smooth surface. After the oxide film is peeled off, the exposed matrix will be further oxidized, making the oxide layer thicker.
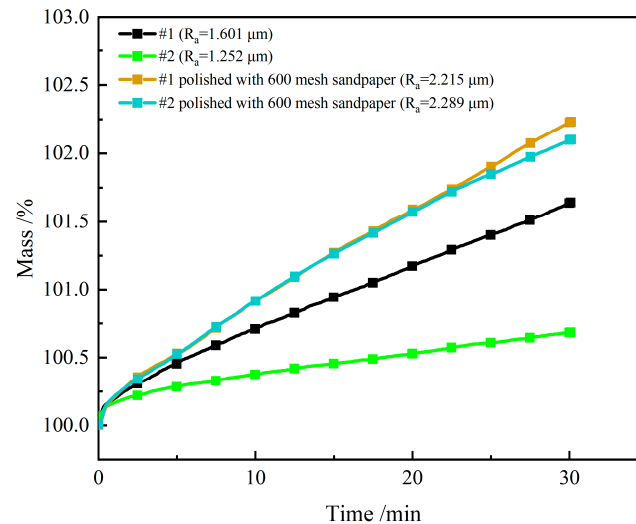

Figure 6. Oxidation weight gain curve of 22MnB5 steel at 920 °C.

In summary, the batch-annealing temperature affects the thickness of the oxide layer during austenitizing by affecting the surface roughness rather than the microstructure of the cold-rolled sheet. Thus, to ensure the mechanical properties, the surface roughness of the cold-rolled plate can be reduced by lowering the batch-annealing temperature during cold rolling, which decreases the oxidation of 22MnB5 steel during hot stamping. However, if the batch-annealing temperature drops sharply, batch annealing will not achieve the desired effect (such as the occurrence of static recrystallization and the release of residual stress), and the microstructure uniformity must be greatly reduced, leading to a decrease in mechanical properties. Therefore, although reducing the batch-annealing temperature may reduce the oxidation phenomenon during austenitizing, considering the microstructure uniformity and mechanical properties, the batch-annealing temperature should be decreased properly. Optimizing the appropriate batch-annealing temperature interval to obtain cold-rolled 22MnB5 steel with satisfactory microstructure and mechanical properties and better surface quality, to reduce the oxidation phenomenon in the hot forming process, and establishing the corresponding model is the focus of subsequent research.

4. Conclusions

Decreasing the batch-annealing temperature from 690 to 680 °C decreased the microstructure uniformity of 22MnB5 steel, but it did not cause an evident decrease in the mechanical properties. The results show that the difference in oxidation is caused by the difference in surface quality rather than the slight microstructure. When the batch-annealing temperature decreased from 690 to 680 °C, the surface roughness of 22MnB5 steel decreased from 1.601 to 1.252 µm, and the oxide thickness of 22MnB5 steel decreased from 58.5 to 41.4 µm. This indicates that properly reducing the batch-annealing temperature decreased the surface roughness, thus reducing oxidation during the austenitizing of 22MnB5 steel without affecting the mechanical properties after quenching.

Author Contributions: Conceptualization, B.L. and X.Z.; methodology, B.L.; software, Y.L.; validation, N.L., J.L. and M.W.; formal analysis, B.L.; investigation, Y.C.; resources, Y.C.; data curation, Y.L.; writing—original draft preparation, B.L.; writing—review and editing, M.W.; visualization, Y.C.; supervision, N.L.; project administration, J.L.; funding acquisition, Y.L. All authors have read and agreed to the published version of the manuscript.

Data Availability Statement: The data presented in this study are available on request from the corresponding author.

Conflicts of Interest: The authors declare no conflict of interest.

References

1. Guo, N.; Zhang, X.; Hou, Z.; Wang, W.; Yang, D.; Min, J.; Ming, P.; Zhang, C. Hot stamping of ultra-thin stainless steel sheets for bipolar plates. *J. Mater. Process. Technol.* **2023**, *317*, 117987. [CrossRef]
2. Gronostajski, Z.; Pater, Z.; Madej, L.; Gontarz, A.; Lisiecki, L.; Lukaszek-Solek, A.; Łuksza, J.; Mróz, S.; Muskalski, Z.; Muzykiewicz, W.; et al. Recent development trends in metal forming. *Arch. Civ. Mech. Eng.* **2019**, *19*, 898–941. [CrossRef]
3. Senuma, T. Hot Stamping Steel. *Encycl. Mater. Met. Alloys* **2022**, *2*, 26–36.
4. Bhadeshia, H.; Honeycombe, R.E. *Steels: Microstructure and Properties*, 4th ed.; Elsevier Ltd.: Amsterdam, The Netherlands, 2017; pp. 271–301.
5. Mori, K.; Bariani, P.; Behrens, B.-A.; Brosius, A.; Bruschi, S.; Maeno, T.; Merklein, M.; Yanagimoto, J. Hot stamping of ultra-high strength steel parts. *CIRP Ann.* **2017**, *66*, 755–777. [CrossRef]
6. Li, B.; Chen, Y.; Zhao, X.; Li, J.; Wang, C.; Wang, M. Effect of Austenitization Process on Oxidative Decarbonization Behavior and Mechanical Properties of 22MnB5 Steel. *J. Mater. Eng. Perform.* 2023, in press. [CrossRef]
7. Yao, Z.; Ma, F.; Liu, Q.; Zhao, F.; Li, F.; Lin, J.; Wang, X.; Song, W. High Temperature Oxidation Resistance and Mechanical Properties of Uncoated Uitrahigh-Strength Steel 22MnB5. In Proceedings of the FISITA 2012 World Automotive Congress, Beijing, China, 27 November 2012.
8. Deng, B.; Yi, H.L.; Wang, G.D. Effect of Mo on high temperature oxidation behavior of 22MnB5 steel sheet during hot stamping. *Steel Roll.* **2020**, *37*, 6–11.
9. Shen, Y.; Ju, Q.; Xu, G.; Du, X.; Zhang, Y.; Zhu, Y.; Huang, J.; Wang, T.; Liu, Z. Improved oxidation resistance and excellent strength of nickel-based superalloy at 1100 °C by determining critical Cr-Al value. *Mater. Lett.* **2022**, *328*, 133226. [CrossRef]
10. Li, F.; Wang, Y.; Dang, W.; Xu, Z.; Zhang, X.; Zhao, K.; Hu, X.; Tang, Y. Polycarbosilane-derived ceramic coatings with crack-free morphology for improving oxidation resistance of steel. *Mater. Lett.* **2022**, *328*, 133088. [CrossRef]
11. Huang, C.-Y.; Chen, Y.; Lin, C.-S. High-temperature oxidation resistance of hot stamping steel with chromium coating electroplated in trivalent chromium bath. *Mater. Today Commun.* **2022**, *33*, 104663. [CrossRef]
12. Chang, J.-K.; Lin, C.-S.; Cheng, W.-J.; Lo, I.-H.; Wang, W.-R. Oxidation resistant silane coating for hot-dip galvanized hot stamping steel. *Corros. Sci.* **2020**, *164*, 108307. [CrossRef]
13. Zhao, Y.; Yang, D.; Qin, Z.; Chu, X.; Liu, J.; Zhao, Z. A novel hot stamping steel with superior mechanical properties and antioxidant properties. *J. Mater. Res. Technol.* **2022**, *21*, 1944–1959. [CrossRef]
14. Mori, K.; Ito, D. Prevention of oxidation in hot stamping of quenchable steel sheet by oxidation preventive oil. *CIRP Ann.* **2009**, *58*, 267–270. [CrossRef]
15. An, L.-Z.; Wang, Y.-P.; Wang, G.-D.; Liu, H.-T. Fabrication of high-performance low silicon non-oriented electrical steels by a new method: Low-finishing-temperature hot rolling combined with batch annealing. *J. Magn. Magn. Mater.* **2022**, *546*, 168907. [CrossRef]
16. Singh, R.K.; Sudharshan, R.; Mehta, P.K.; Chandrawanshi, M.; Mishra, D. Optimization of annealing stack using design of experiment method in Batch Annealed HSLA Steel. *Mater. Today Proc.* **2018**, *5*, 7055–7060. [CrossRef]
17. Kumar, D.; Viswanathan, N.N.; Sarkar, P.S. Heat Transfer Model of Coil in a Bell Annealing Furnace. In *Proceedings of Recent Advances in Manufacturing Processes and Systems, Lecture Notes in Mechanical Engineering*; Springer: Singapore, 2022.
18. Tamer, J.; Ozgultekin, G.; Poyraz, O.; Seyalioglu, C. Formability Analyses of a Novel Alloy Cold-rolled Batch Annealed Dual Phase Steel. *Procedia Manuf.* **2020**, *47*, 1211–1216. [CrossRef]
19. Zhao, X.L.; Chen, W.; Zhao, Z.Z.; Wang, S. Effects of Batch Annealing Temperature on Microstructure and Mechanical Properties of 1500 MPa Grade Hot Stamping Steel. *Hot Work. Technol.* **2022**, *51*, 149–156.
20. Tong, C.; Yardley, V.A.; Shi, Z.; Rong, Q.; Li, X.; Zhang, B.; Xu, D.; Lin, J. Investigation of the effect of initial states of medium-Mn steel on deformation behaviour under hot stamping conditions. *Mater. Sci. Eng. A* **2022**, *855*, 143914. [CrossRef]
21. Miadad, S.J.; Venugopalan, T.; Halder, N.; Kumar, B.R. On the Study of Batch Annealing Parameter Optimization for Higher Lankford Value in High Phosphorus Interstitial Free High Strength Steel. *J. Mater. Eng. Perform.* **2020**, *29*, 7598–7606. [CrossRef]
22. Steineder, K.; Krizan, D.; Stadler, M.; Ritsche, S.; Berger, E.; Holtmann, N.; Schnitzer, R.; Schneider, R. Critical Aspects Concerning Large-scale Production of a Batch-annealed Medium-Mn 780 MPa Grade for Automotive Applications. *Berg-Huettenmaenn. Monatsh.* **2022**, *167*, 513–516. [CrossRef]
23. Han, J.; Neupane, S.; Wang, L.; Seyeux, A.; Klein, L.; Zanna, S.; Mercier, D.; Maurice, V.; Marcus, P. Effect of surface preparation by high-temperature hydrogen annealing on the passivation of Ni-20 at.% Cr alloy in sulfuric acid. *Electrochim. Acta* **2023**, *454*, 142403. [CrossRef]
24. González-Leal, J.M.; Gallero, E.; Blanco, E.; del Solar, M.R.; Nuñez, A.; Almagro, J.F. Analysis of the Visual Appearance of AISI 430 Ferritic Stainless Steel Flat Sheets Manufactured by Cool Rolling and Bright Annealing. *Metals* **2021**, *11*, 1058. [CrossRef]

25. Fang, G.; Jin, W.; Pei, G.; Yong, T.; Yang, Y. Analysis to the Application of Hydrogen Bell-Type Annealing Furnace in Baosteel Stainless Steel. In Proceedings of the PRICM: 8th Pacific Rim International Congress on Advanced Materials and Processing, Waikoloa, HI, USA, 4–9 August 2013.

26. Cui, G.Y.; Wang, Y.; Wang, G. Process optimization and performance analysis of batch annealing for low carbon cold rolled sheet. *Steel Roll.* **2018**, *35*, 90–93.

27. Humphreys, J.; Rohrer, G.S.; Rollett, A. *Recrystallization and Related Annealing Phenomena*, 3rd ed.; Elsevier Ltd.: Amsterdam, The Netherlands, 2017; pp. 527–567.

28. Birks, N.; Meier, G.H.; Pettit, F.S. *Introduction to the High-Temperature Oxidation of Metals*; Cambridge University Press: Cambridge, UK, 2006.

29. Wang, L.; Jiang, W.-G.; Li, X.-W.; Dong, J.-S.; Zheng, W.; Feng, H.; Lou, L.-H. Effect of Surface Roughness on the Oxidation Behavior of a Directionally Solidified Ni-Based Superalloy at 1100 °C. *Acta Met. Sin. (Engl. Lett.)* **2015**, *28*, 381–385. [CrossRef]

30. Cheng, C.-Q.; Hu, Y.-B.; Cao, T.-S.; Zhang, L.; Zhu, Y.-W.; Zhao, J. Two typical oxidation models on nickel-based superalloys under different initial surface roughness. *Corros. Sci.* **2020**, *176*, 108942. [CrossRef]

31. Platt, P.; Allen, V.; Fenwick, M.; Gass, M.; Preuss, M. Observation of the effect of surface roughness on the oxidation of Zircaloy-4. *Corros. Sci.* **2015**, *98*, 1. [CrossRef]